

## Droplets Splash Related with a Wall Impingement of Liquid Jet 액체 분무의 벽면 충돌분무에 의한 액적 비산

김 영 일\*  
Young-II KIM\*

### <요 약>

벽면에 충돌하는 액체 분무의 충돌 거동과 액적 비산에 관하여 실험을 통하여 조사하였다. 액체 분무는 홀노즐에 의해 직경 40mm의 충돌판에 분사하게 된다. 액체 분무는 반경방향으로 퍼져나가 5개의 영역으로 분류되어 나타내게 된다. 난류 혹은 층류 분무의 경우, 충돌판에 충돌한 후 두꺼운 액막을 형성하게 되며, 이러한 상태에서 충돌하는 분무의 비산량은 매우 적으며 충돌 거리에 영향을 받지 않는다. 한편, 파동이 있는 분무의 충돌은 수력도약(Hydraulic jump)과 함께 반경방향으로 얇은 액막을 형성하게 되며 비산율도 증가하게 된다. 액체분무의 초속도가 증가하면 비산율도 증가하게 된다. 분열이 일어난 후에 충돌하는 파동 분무의 비산율은 분열이 일어나기 전에 비해 약 2~3 배 정도 크게 나타난다. 비산율은 웨버수(Weber number)를 이용하여 요약할 수가 있다.

**Key words** : *Liquid jet, Wall impingement, Break-up length, Splash ratio, Weber number*

### 1. INTRODUCTION

In recent years, it has been required to develop a small type diesel engine or spark ignited direct injection gasoline engine for fuel economy of an automotive. In a direct injection engine, fuel was injected directly into cylinder of the engine. Then, some amount of injected fuel impinged on a wall of the combustion chamber. On the other hand, in a port fuel injection system of SI

engine, a fuel injected through an EFI nozzle was impinged on an inner wall of the manifold or an upper surface of the intake valve. Some amount of injected fuel was scattered from the impingement point and formed into a fine droplet spray. Therefore for both of ID diesel and SI engines, it is important to understand fuel dispersion and spray behavior on the wall.

In a port fuel injection system of SI engine, fuel behavior both in the intake port and in the cylinder has significant influence

---

\* 정회원, 대천대학 자동차기계학부 조교수·공학석사  
일본 群馬大學 대학원 박사과정 수료  
355-830, 보령시 주포면 관산리 산6-7  
E-mail yikim@dcc.ac.kr

on the transient A/F characteristics and HC emissions. Then, fuel flow and fuel spray on the wall or in the intake port had been studied<sup>1-4)</sup> to develop the effective supplying method of fuel. The fundamental approach to understand the impingement phenomena of liquid jet had been started from studies of a single droplet impingement<sup>5-6)</sup> and formation of liquid film on a surface<sup>7)</sup>. As for a single droplet impingement process, a lot of experimental and theoretical works had revealed a deformation process of droplet at an instance of impingement. In a mixture formation process in a DI diesel engine, fuel spray was also impinged on a cavity wall of combustion chamber, and heat release during combustion process was greatly affected by this impingement process<sup>8)</sup>. Impingement of diesel spray on a wall was experimentally studied and also numerically analyzed<sup>9-12)</sup>. However, it needs more detail information to utilize effectively a wall impingement process for high efficiency engine.

In this study, to find out a relationship between liquid jet impingement and reflecting or scattering behavior of droplets, fundamental behavior of liquid jet impingement was experimentally investigated. The splash ratio was defined with a ratio of splashed liquid to the total injected liquid. It was discussed with an impingement distance and impingement velocity of a liquid jet.

## 2. EXPERIMENTAL SET-UP and IMPINGEMENT SYSTEM

Experimental set-up to investigate impingement behavior of a laminar or turbulent jet on a smooth surface is shown in Fig.1. Test liquid was tap water. It was supplied from a pressurized water tank to a test nozzle. Test nozzle was made of straight pipe of stainless steel. A target wall for impingement was a smooth surface of aluminum plate. Flow rate was regulated by a valve and monitored by a flow meter. Impingement behavior of a liquid jet was observed by a stroboscope and camera system. A liquid film, which was formed on a plate surface, flowed and dripped down from the periphery of plate as showed in the figure. To capture the dripping water from the periphery of plate, a vacuum pump and balance system was used. An electric needle probe was used to measure the thickness of a water film on the plate and to measure a radial position of the hydraulic jump mentioned later.

Figure 2 shows detail construction of the target plate and the plate holder. To

enhance the smooth dripping of liquid film into the plate holder, annular slit between the plate and the plate holder, and the edge angles were designed according the results of preliminary experiment. From photographic observations of the dripping phenomena of liquid, it was founded that the annular slit of 3mm and the edge angles of 30 degrees were enough for effective capture of film water on the impingement surface. Test nozzle was produced as becoming  $L_n/D_n=50$ . Distance from nozzle to target surface of plate was  $Z_p$ .

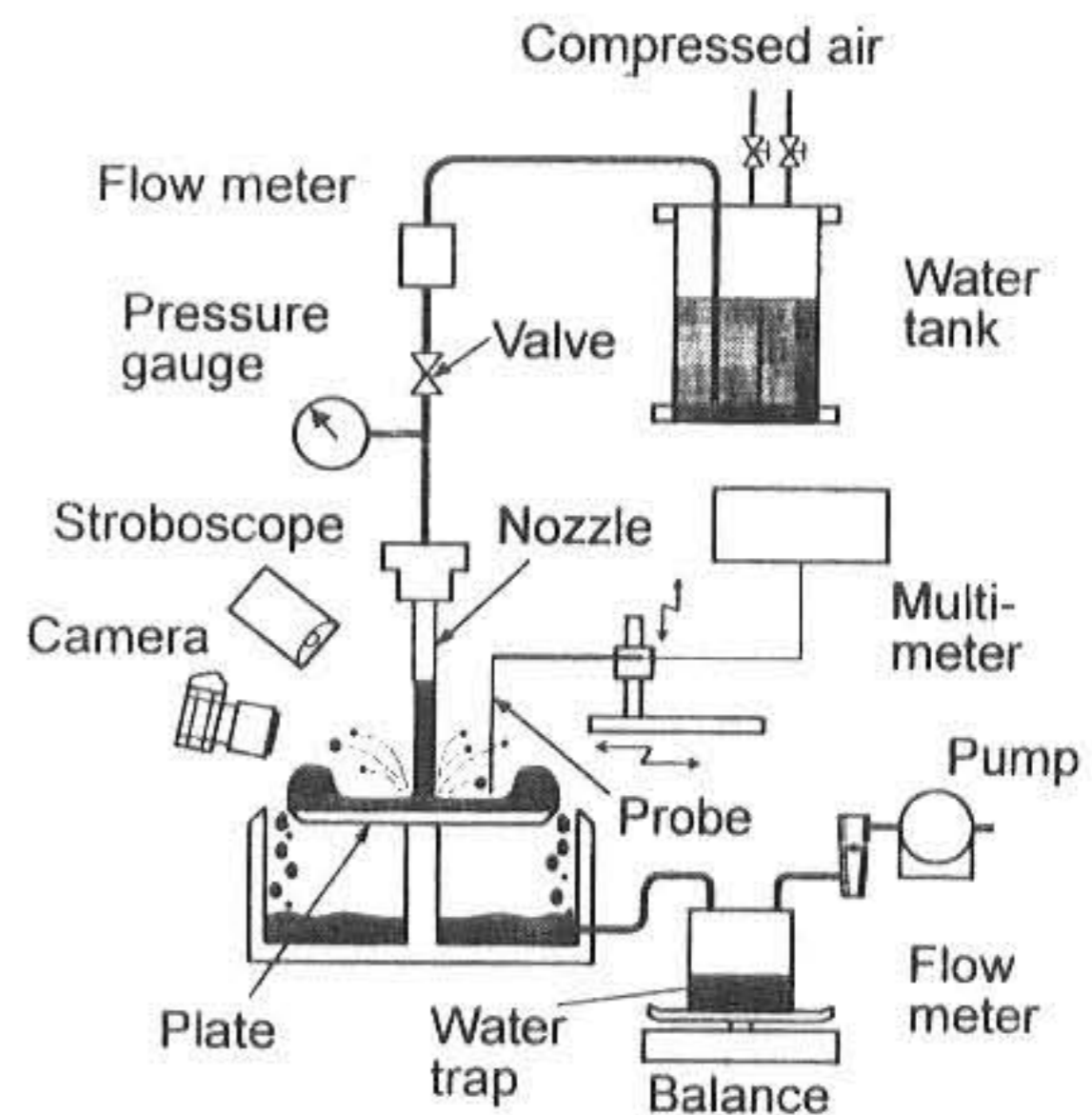


Fig.1 Experimental set-up

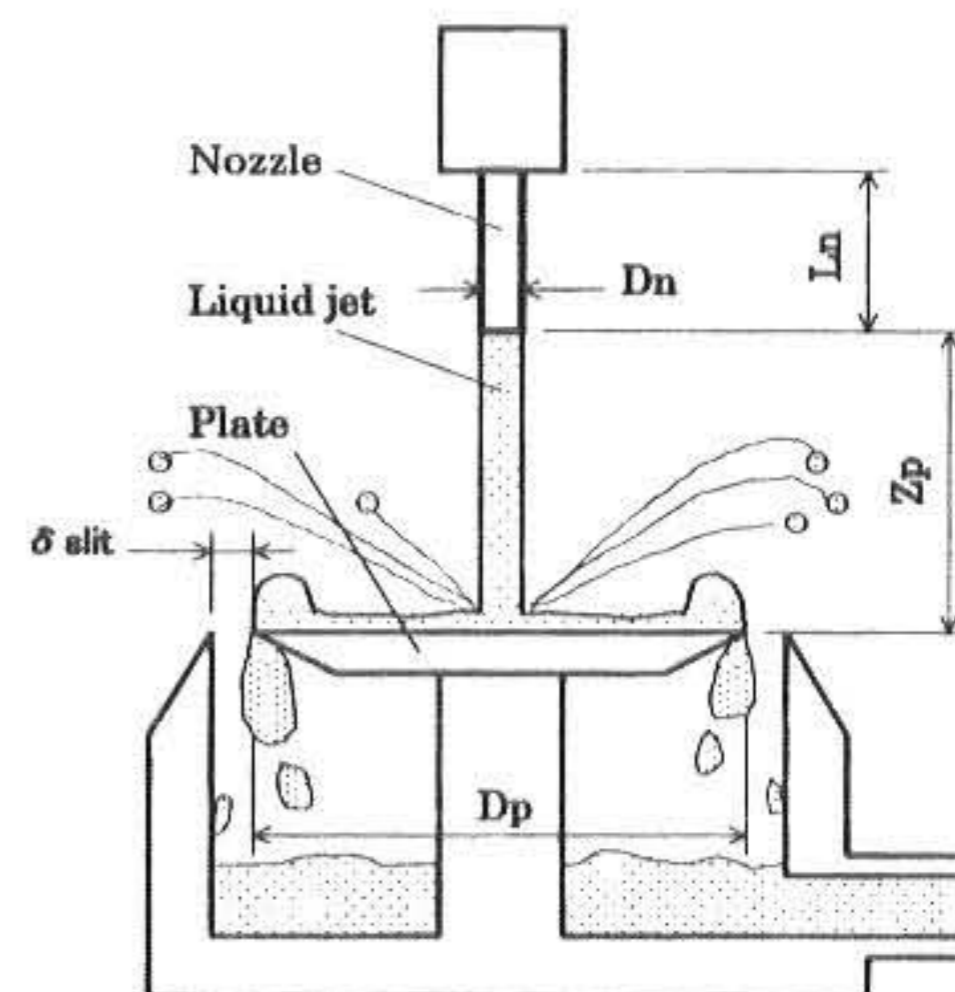


Fig.2 Nozzle and impingement system

A liquid jet impinging on the plate was divided into droplets and liquid falling in to the vessel after forming a liquid film. A splash ratio of droplets was defined by the ratio of splashed liquid mass to the total injected liquid mass. It was obtained from total of injected liquid and amount of liquid captured in the vessel by using the following

formula;

$$\varepsilon_s = \frac{Q_{splash}}{Q_{total}} = \frac{Q_{total} - Q_{film}}{Q_{total}}$$

where  $s$  is splash ratio,  $Q_{total}$  is the amount of total injection,  $Q_{film}$  is the amount of collected liquid and  $Q_{splash}$  is the amount of splash.

### 3. IMPINGEMENT BEHAVIOR and BREAK-UP LENGTH

#### 3.1 Impingement behavior

The flow patterns on the plate and splashment of droplets could be classified into five regions by the impingement behavior of the jets. The classifications indicated by Regions I-V were corresponding to the flow patterns shown in Fig. 3. When the liquid velocity was low and the jet was laminar, a smooth liquid surface indicated by Region I was observed on the plate. The flow pattern on the plate was not affected by the position of the plate. Even if the plate was far away from the nozzle and droplets array was impinged, the flow pattern was not changed. Impingement of the liquid jet of transient jet between laminar and wavy jets, formed the liquid flow indicated by Regions II and III. Flow pattern of Region II was characterized by a smooth surface with bubble containing flow.

A hydraulic jump and a little amount of splashed droplets were the special feature of the state of Region III.

Impingement pattern of the wavy jet was characterized by the thin film and splashed droplets. The flows in Region IV was modeled by a film flow with liquid rim and splash of droplets. When the velocity of the jet was too high to make the rim on the periphery of the plate, flow pattern was changed to Region V which was simply characterized by a thin film with the splashment of droplets. The thickness of this water film on the plate was less than 1mm and it was not effected by the impingement velocities of the jets in regions III, IV and V.

#### 3.2 Break-up length and flow mode on a plate

The flow state in a nozzle characterized a liquid jet injected from the nozzle. The laminar flow usually made a smooth jet and the turbulent flow resulted in a wavy jet. These states of a jet and a distance from nozzle characterized the liquid jet at an impingement point. A liquid jet that was

$$D_n = 1.19 \text{ mm} \quad L_n/D_n = 50 \quad D_p = 40 \text{ mm} \quad z_p = 30 \text{ mm}$$

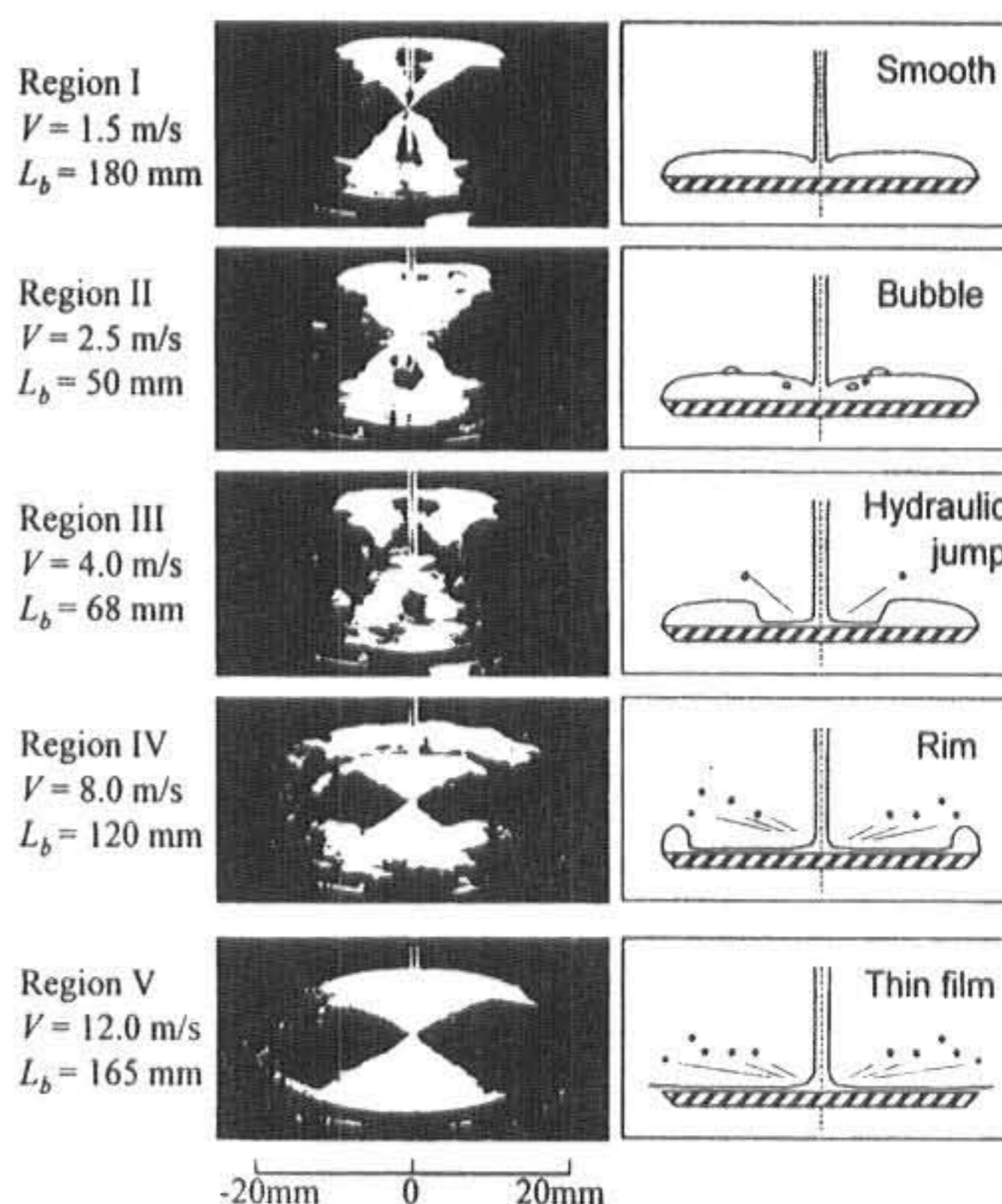


Fig.3 Impingement behavior of a liquid jet observed near the nozzle exit was

continuous liquid jet. However, the liquid jet, which was observed far down stream of its break-up length, was droplets array or spray. Then the impingement phenomena of a jet had to be discussed with the characteristics of jet and with the distance from a nozzle to a target plate. To discuss them, the break-up length and impingement behavior of a liquid jet in  $D_n=0.49\text{mm}$  were summarized and shown in Fig. 4. The volumetric average velocity in the nozzle was adapted and Reynolds number of the jet was based on this average velocity, nozzle diameter and kinetic viscosity of the water. The classifications indicated by Region I-IV in the figure were corresponding to the flow patterns shown in Fig. 3. Impingement phenomena of a smooth jet was corresponding to the Region I. And before and after break-up of a smooth jet gave no influence on the flow pattern on the plate. However, when the jet was in the transient state, the break-up behavior gave a change of flow pattern on the plate. The impingement flow pattern indicated by Region III appeared in the wavy jet region. At higher injection velocity, impingement flow pattern changed from Region III to Region IV and this change was also affected by the distance from the nozzle to the target plate.

Figure 5 shows the break-up length and impingement behavior of a liquid jet in  $D_n=1.19\text{mm}$ . In this case, Region V

appeared on a wavy jet of high velocity. In Figs. 4 and 5, the border between Regions III and IV had same tendency. All the borders of the flow patterns were sited on the almost same flow domains when the flow domains were summarized by the Reynolds number. It meant that the turbulence level of the jet was one of the main factors of the impingement behavior.

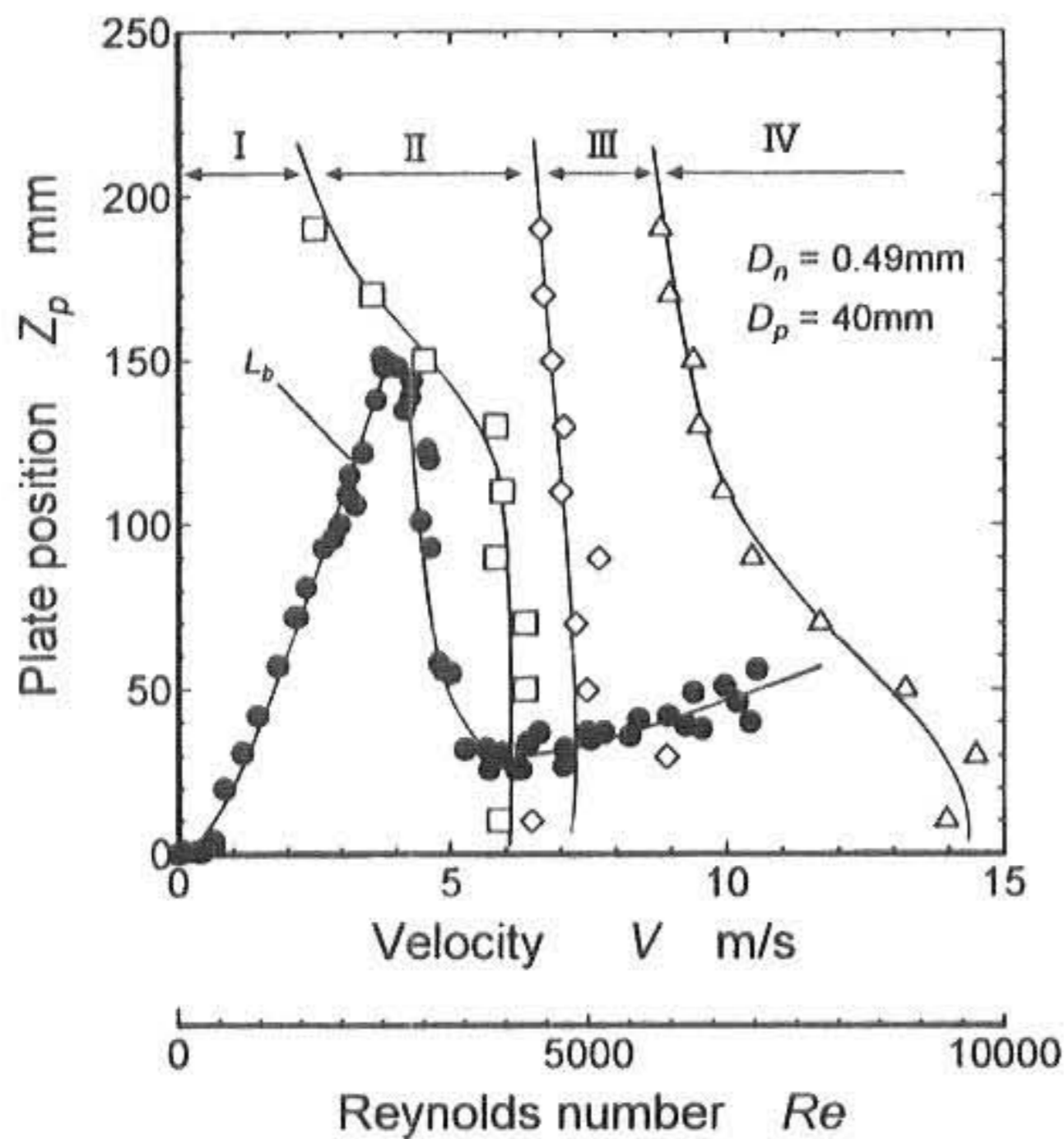


Fig. 4 Break-up length and impingement behavior of a liquid jet ( $D_n=0.49\text{mm}$ )

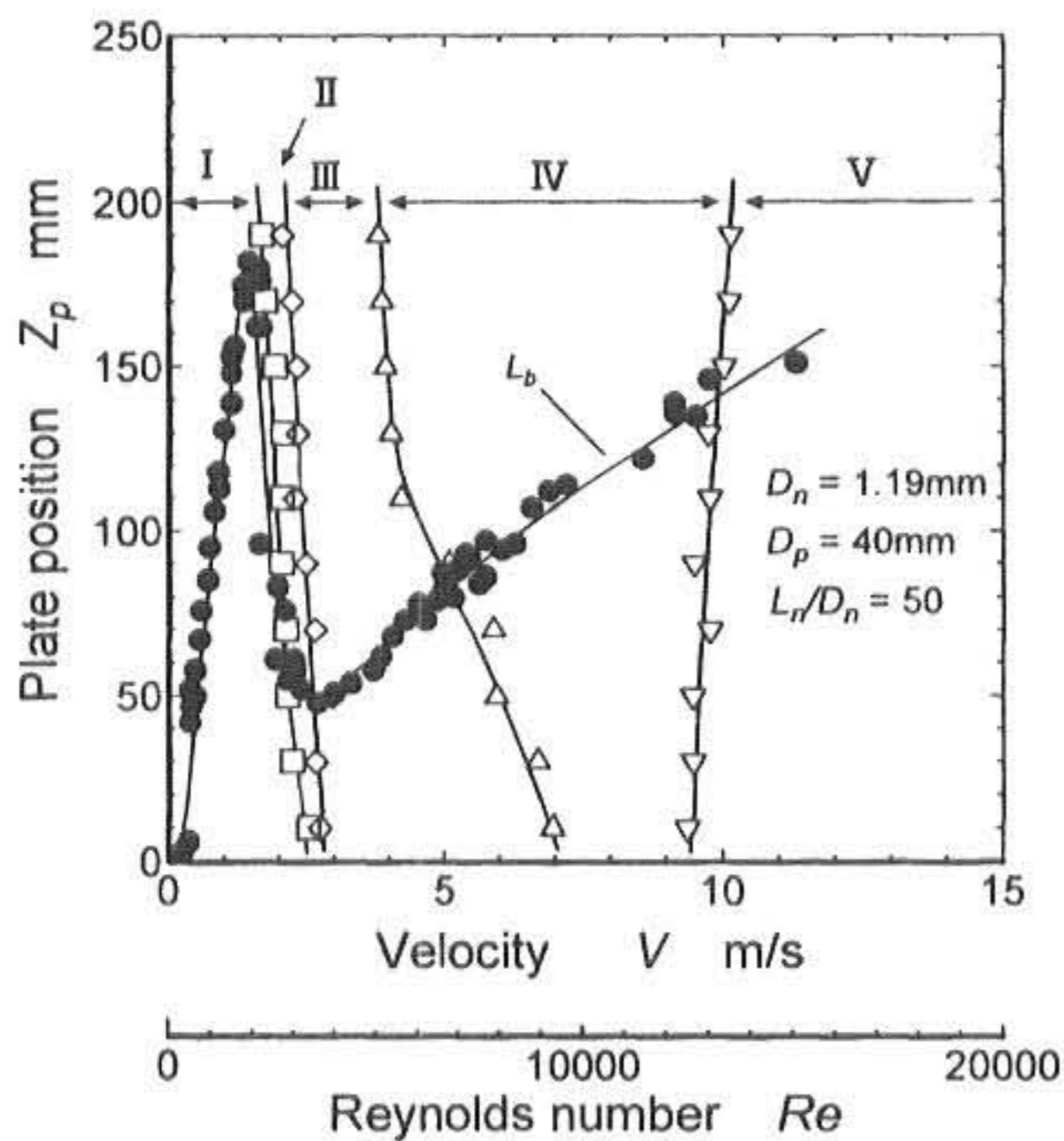


Fig. 5 Break-up length and impingement behavior of a liquid jet ( $D_n=1.19\text{m}$ )

### 3.3 Hydraulic jump

Figure 6 shows the relation between nozzle diameter and velocity at which the

hydraulic jump phenomenon took place on the impingement plate. In this relationship, the onset of the hydraulic jump was checked on the plate which was positioned at  $Z_p=70\text{mm}$ . Further, the onset velocity of the wavy flow is also shown in this figure. When the jet diameter became larger, the kinetic energy of the jet also became larger, and the hydraulic jump phenomenon could be observed at lower velocity. In addition, comparing with onset of wavy flow, the onset of the hydraulic jump was observed at a little slow but almost same velocity. In other word, the hydraulic jump could not be observed on the impingement of a laminar jet.

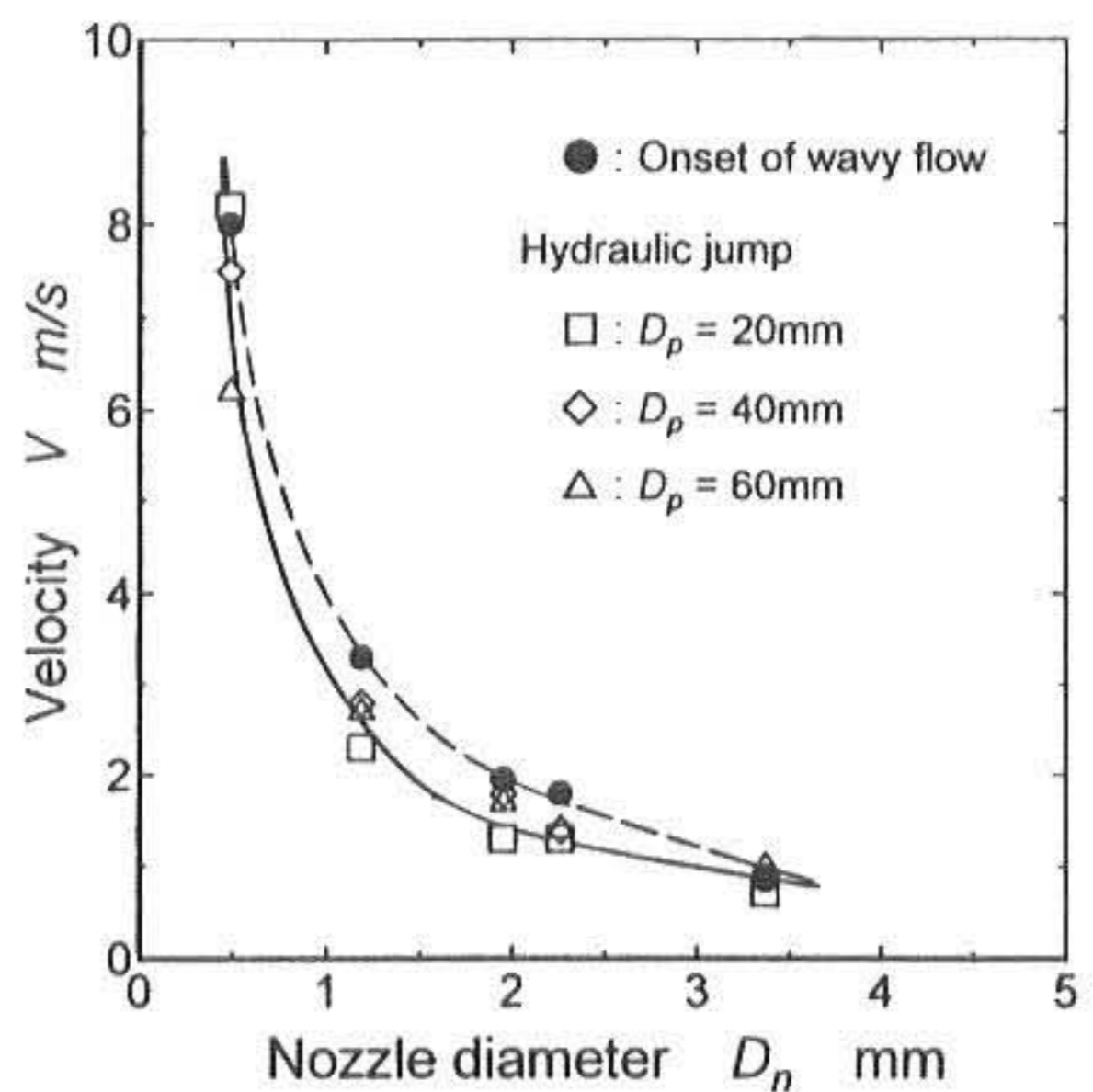


Fig. 6 Effect of nozzle diameter on a velocity of hydraulic jump

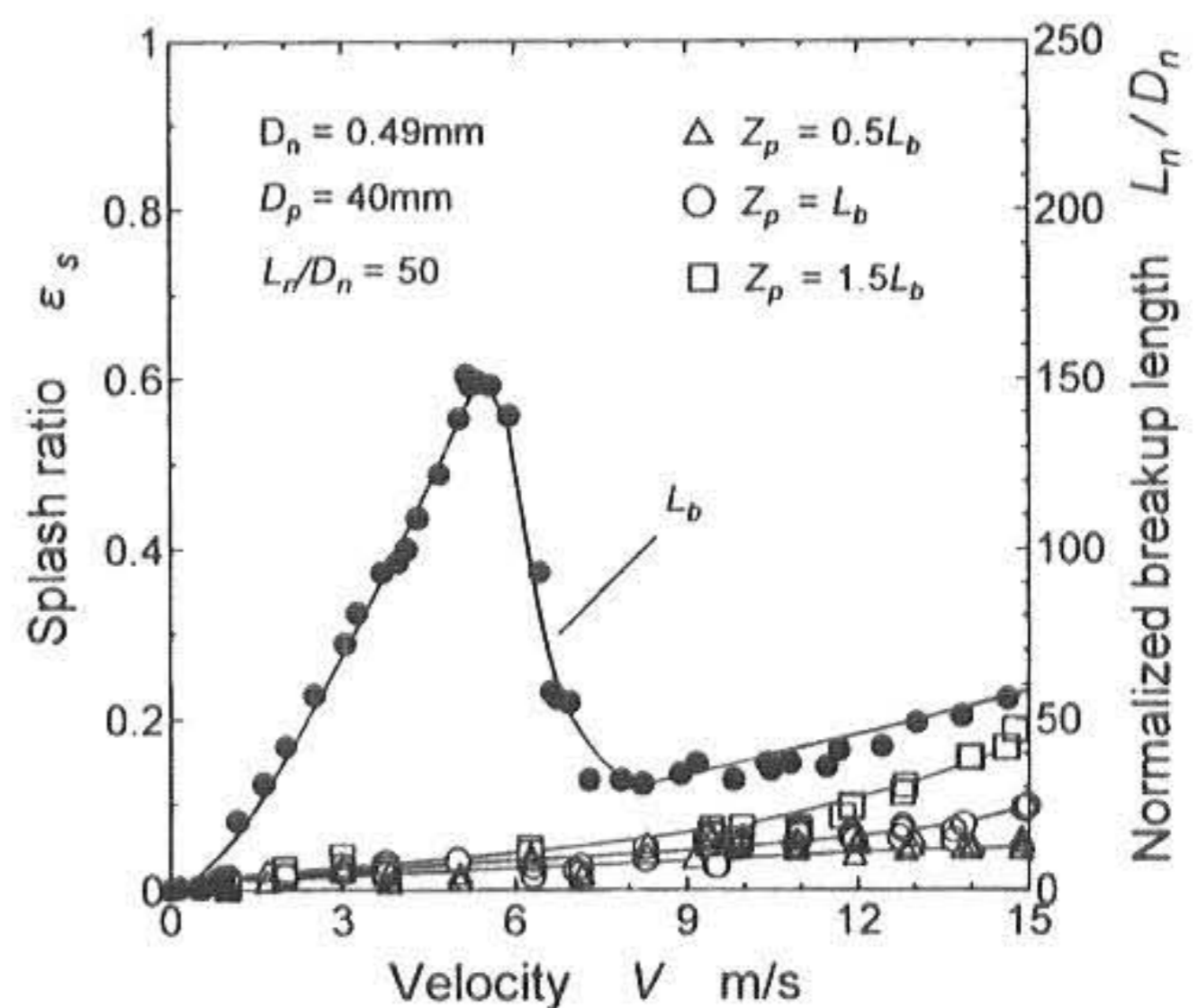


Fig. 7 Effects of velocity and impingement position on a splash ratio of droplets ( $D_n=0.49\text{mm}$ )

## 4. SPLASH RATIO of DROPLETS

### 4.1 Break-up length and splash ratio

Liquid jets of before and after break-up were different in impingement behavior. Then, the relation between splash ratio of droplets and break-up length of the liquid jet could be discussed using the results shown in Figs. 7 and 8. The splash ratios in Fig. 7 were measured at  $Z_p=0.5L_b$ ,  $Z_p=L_b$ (break-up position),  $Z_p=1.5L_b$  for every impinging liquid jet. The splash ratio increased smoothly with an increase of injection velocity and with an increase of impingement distance of the liquid jet. In spite of flow transition from smooth jet to wavy jet, there was no particular change of splash ratio.

The results of  $D_n=1.19\text{mm}$  are shown in Fig. 8. Splash ratio became higher than the case of  $D_n=0.49\text{mm}$ . The increment of the splash ratio was obvious in the wavy jet region. Further, the splash ratio of after break-up jet ( $Z_p=1.5L_b$ ) was larger than the splash ratio measured at  $Z_p=0.5L_b$ . It was considered that the disintegrated liquid jet or droplets array formed from a turbulent jet gave stronger impact to the impingement point than the other conditions and its impact force promoted the splashing.

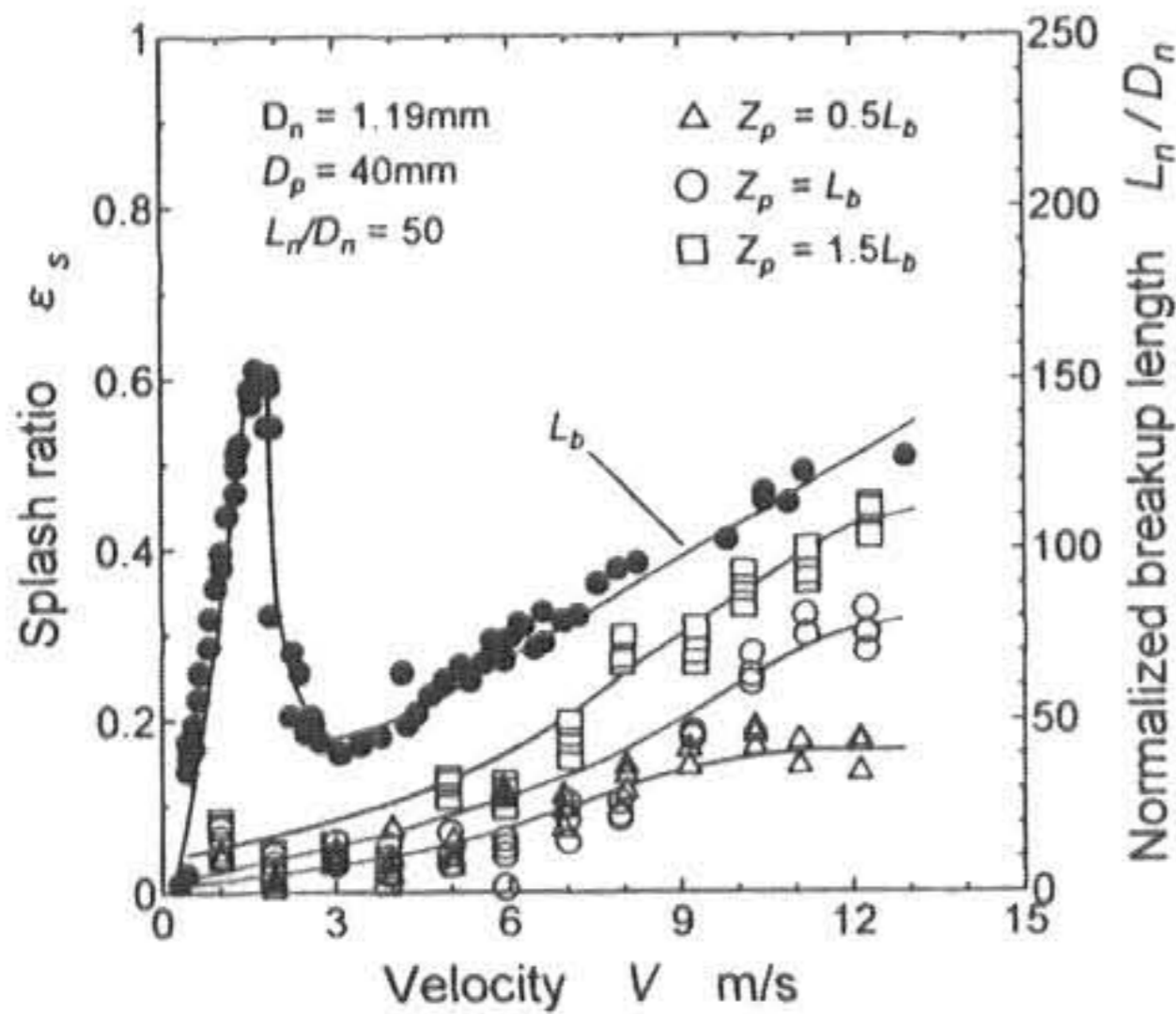


Fig.8 Effects of velocity and impingement position on a splash ratio of droplets ( $D_n=1.19\text{mm}$ )

The splash ratios of transition jets injected from various nozzles are shown in Fig. 9. Even in the distance from the nozzle to the impingement plate becomes longer, no particular increase in the splash ratio resulted in. From the results shown in Figs. 4 and 5, impingement pattern was changed from Region I to Region II with an increase of the injection velocity in the transition jet. And also the impingement distance changed the impingement flow pattern. However these changes had no influence on the splash ratio and the splash ratio was remained in low. It was

considered that the thick radial flow with smooth surface was not basically splashing the liquid.

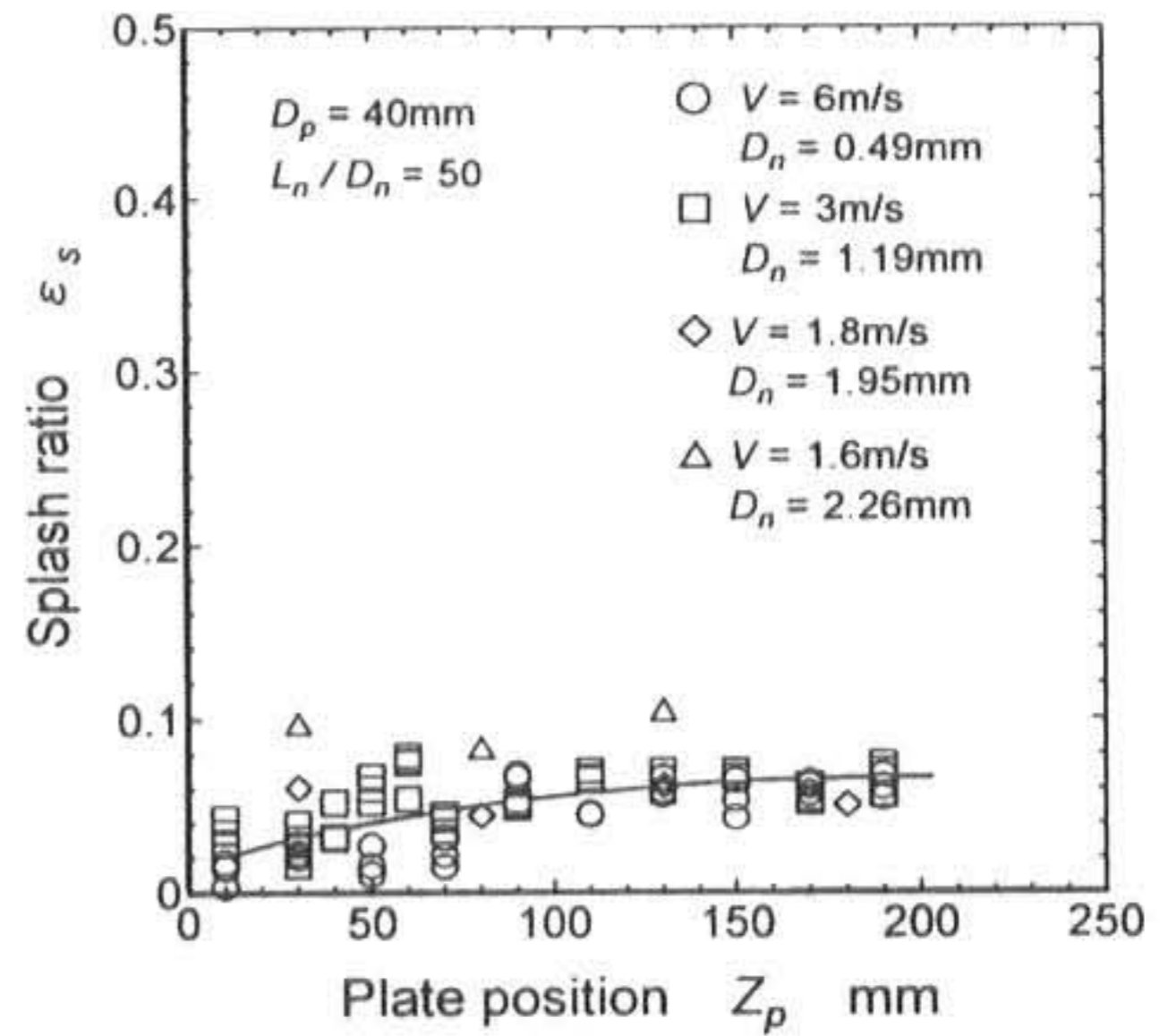


Fig.9 Splash ratios of transition jets injected from various nozzle

#### 4.2 Jet Weber number and splash ratio

When the impingement plate position becomes more distant from the nozzle, the fluctuation of the surface of the liquid jet at the impingement position becomes stronger and its makes the disintegration of the jet if the distance is larger than the break-up length. The Weber number having the jet diameter as representation length was generally used to express the instability of liquid jet. However, for this splash phenomena, the Jet Weber number  $We_j$  having the impingement distance  $Z_p$  for the representation length was used as a dimensionless number showing instability of the liquid jet at impingement point. In this study, Jet Weber number was defined as follow

$$We_j = v \sqrt{\frac{\rho Z_p}{\sigma}}$$

where  $\sigma$  is the surface tension of liquid and  $\rho$  is the density.

The relation between the Jet Weber number and the splash ratio was obtained at several distance of  $Z_p$ . The results obtained for the nozzle of  $0.49\text{mm}$  diameter is shown in Fig. 10. The splash ratio was well correlated with the Jet Weber number and it increased with the Jet Weber number. The results concerning the nozzle of  $D_n=1.19\text{mm}$  is shown in Fig. 11. The splash ratio of various impingement positions increased with an increase of the Jet Weber number. And also it seems that the Jet Weber number uniquely expressed the

splash ratios of different impingement positions.

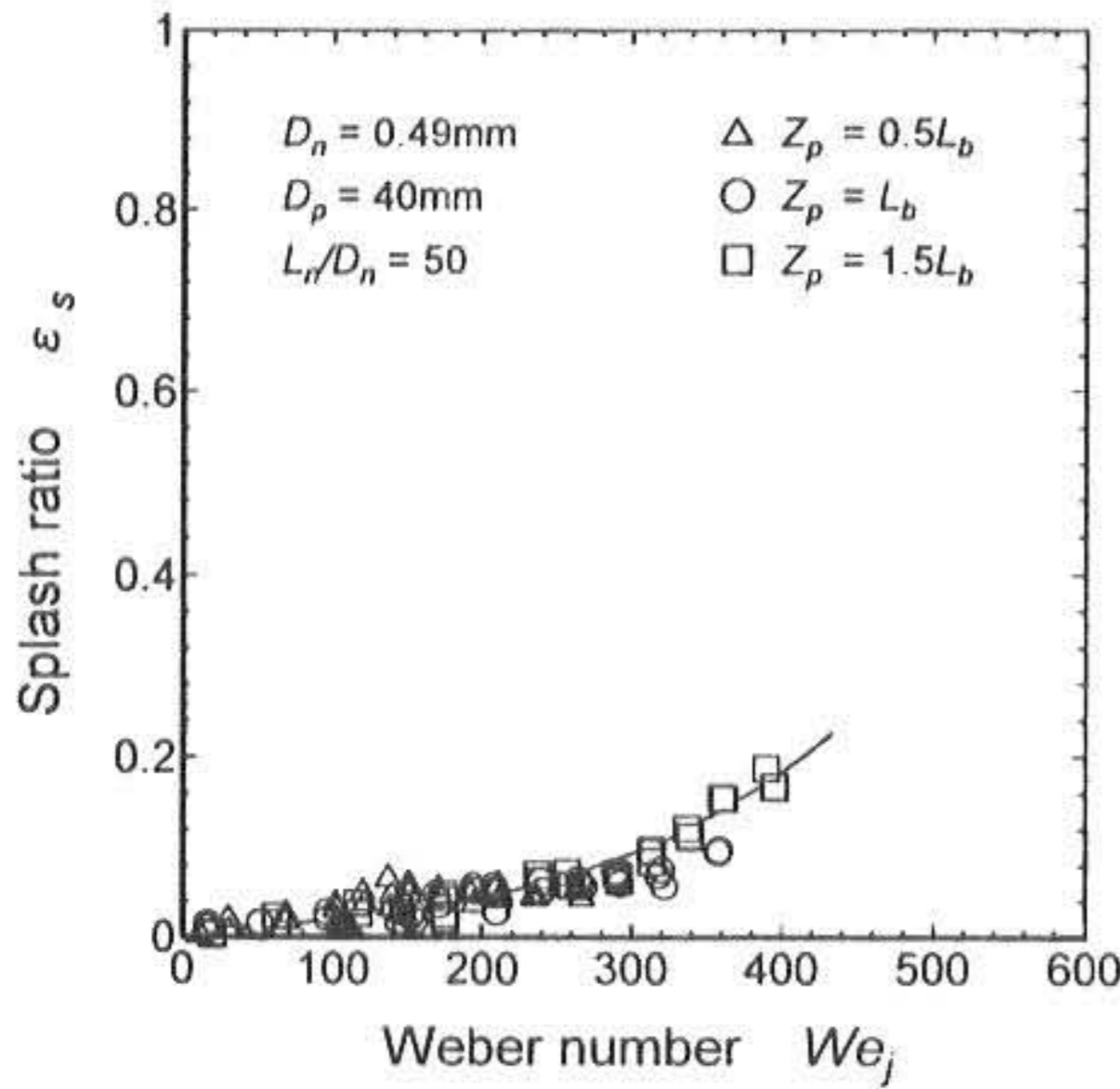


Fig.10 Effect of Jet Weber number on splash ratios of various impingement positions ( $D_n=0.49\text{mm}$ )

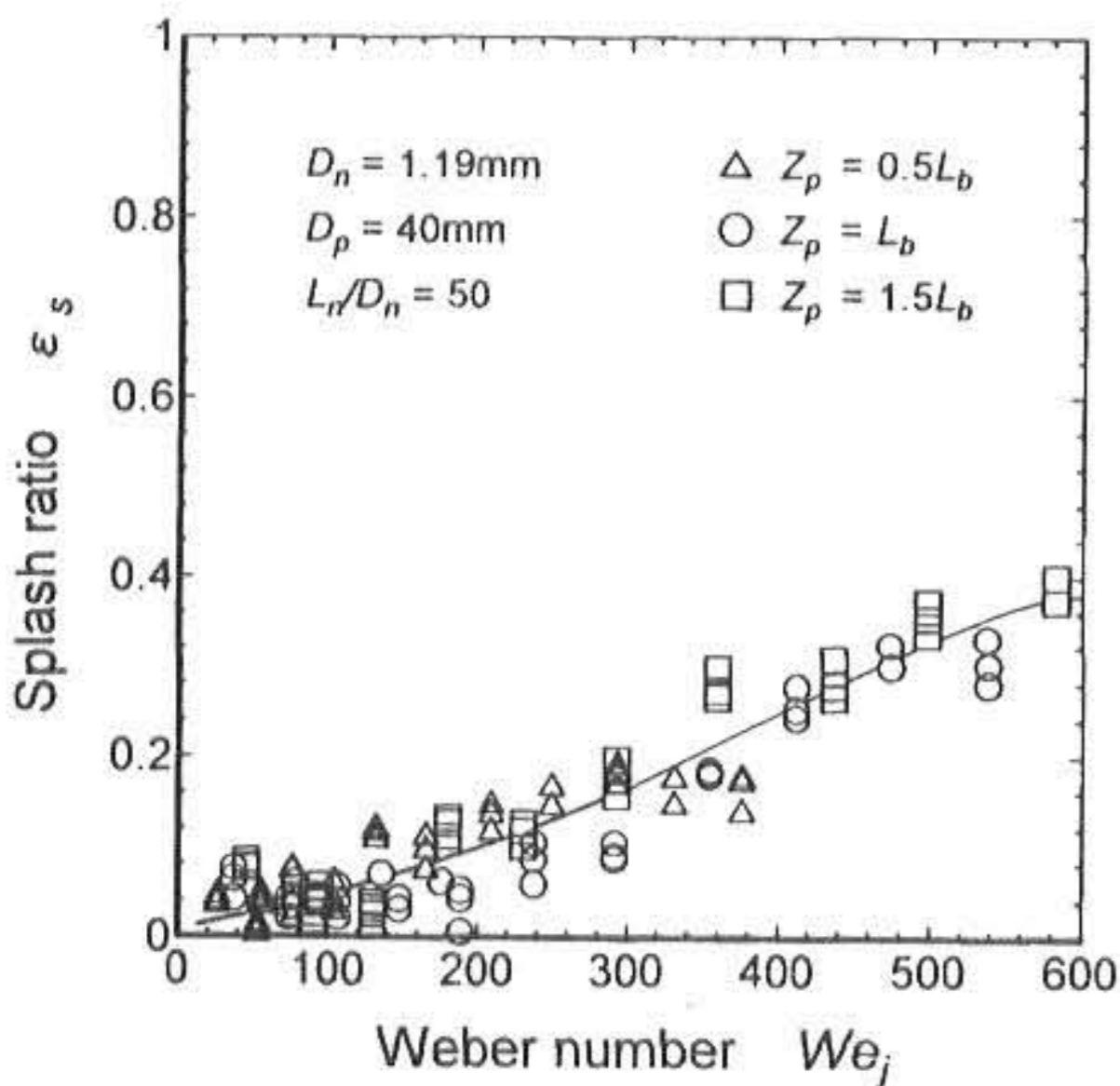


Fig.11 Effect of Jet Weber number on splash ratios of various impingement positions ( $D_n=1.19\text{mm}$ )

Based on the results so far, we could see that the splash ratio increased when the impingement length of the liquid jet became longer than the break-up length of the liquid jet. At the break-up point of the jet, it seems that kinetic energy of the disturbance was enough to disintegrate the jet and it caused the splashment if it was impinged on a plate. Therefore, the Jet Weber number  $We_j(Z_p=L_b)$  and the splash ratio  $\epsilon_s(Z_p=L_b)$  obtained at break-up position become the standard levels to normalize the results of various velocity jets injected by various nozzles of different diameters. Figure 12 shows the summarized results of non-dimensional splash ratio. If the impingement is set at a shorter distance

than the break-up length, the splash ratio does not so much increase. However, the obtained result reveals that the splash ratio rapidly increases when the impingement is set at a longer distance than the break-up length.

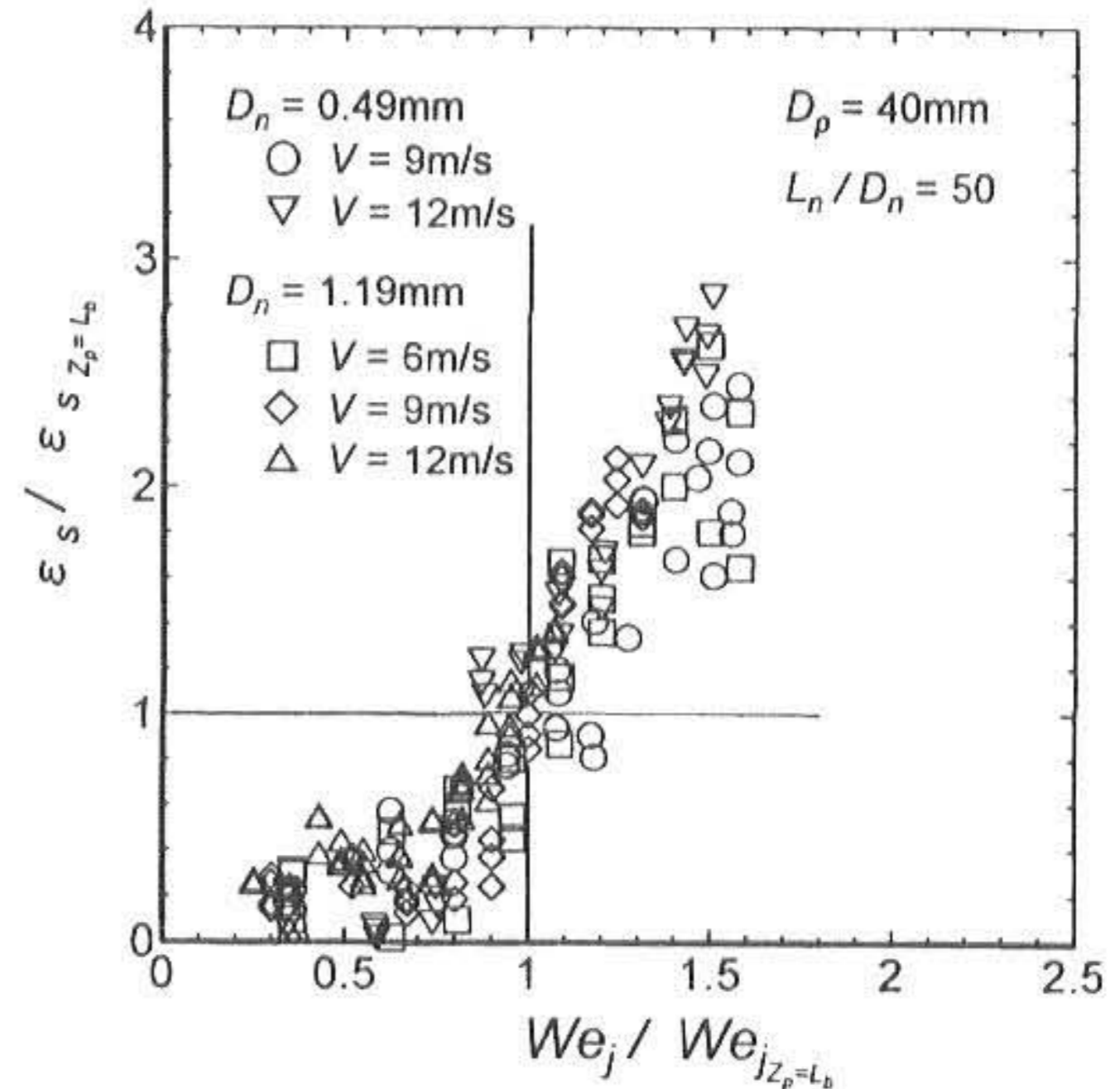


Fig.12 Normalized splash ratios of various wavy jets

### 5. CONCLUSIONS

The fundamental study on wall impingement phenomena of a liquid jet was performed. The splash ratio and reflecting or scattering behavior of droplets were introduced as the impingement characteristics of jet. Then, the results were summarized as follows:

1. Impingement phenomena were classified into following five regions. (a) smooth surface flow, (b) bubble containing flow, (c) flow with hydraulic jump, (d) film flow with rim and droplet splash, and (e) thin film flow with droplets splash.
2. The splash ratio of the wavy jet is larger than that of laminar flow jet.
3. In case of the wavy jet, the splash ratio of after break-up impingement was larger than that of before break-up impingement.
4. As a result from application of the Jet Weber number, the effect of fractionation which affects to the splash ratio could be clarified.

### REFERENCES

1) Keiso Takeda, et. al. : Mixture Preparation and HC Emissions of a 4-Valve Engine with Port Fuel Injection During Cold Starting and Warm-up, SAE Paper

950074, 1995.

2) Y.Hosho, H.Nakai and T.Kadota, "Transient Fuel Supply Characteristics in a Carburetted SI Engine under Accelerating Conditions", Proc. of Int. Symp. of Diagnostics and Modeling of Combustion in Internal Combustion Engine, 1985, 91-98.

3) P.O.Witze and R.M.Green, "Techniques for Enhancing the Observation of PFI Spray Patterns in a Bench-Top Spray Rig", Proc. of 4th Int. Symp. of Diagnostics and Modeling of Combustion in Internal Combustion Engine, 1998, 511-516.

4) S.Lee et. al, "A Comparison of Fuel Distribution and Combustion During Engine Cold Start for Direct and Port Fuel Injection System", SAE Paper 1999-01-1490.

5) A. SAITO and K, KAWAMURA, "Behavior of Fuel Film on a Wall at Fuel Spray Impingement", Proc. of ICLASS-'97, Vol.2, (1997), 54-61

6) J. Fukai, et. al., Phys. Fluid A, Vol.5, No.11, pp.2588-2599, (1993).

7) K.Araki and A. Moriyama, Proc. of ICLASS-82, pp.389-396, (1982).

8) L.Zhang, et. al. "Observation and Calculation of the Combustion Characteristics of a HSDI Engine : Effects of Combustion Chambers and Injection Specifications", Proc. of 4th Int. Symp. of Diagnostics and Modeling of Combustion in Internal Combustion Engine, 1998, 45-49.

9) S.P.Mislevy and P.V.Farrell, "Spray Characteristics of an Impinged Diesel Fuel Spray", Proc. of ICLASS-'97, Vol.2, (1997), 231-238

10) T.Ebara, K.Amagai and M.Arai, "Movement and Structure of Diesel Spray Impinging on a Inclined Wall", SAE Paper No.970046.

11) T.Ebara, K.Amagai and M.Arai, "Penetration Model of a Diesel Spray along a Wall", Proc. of 4th Int. Symp. of Diagnostics and Modeling of Combustion in Internal Combustion Engine, 1998, 423-428.

12) J.Senda, et.al, "Modeling Spray Impingement Considering Fuel Film Formation on the Wall", SAE Paper No.970047.

(2003년 10월15일 접수, 2004년 2월20일 채택)